Electrical control of 180° domain walls in an antiferromagnet

Special Collection: Emerging Materials in Antiferromagnetic Spintronics

O. J. Amin ✉ ⓘ ; S. Reimers; F. Maccherozzi; S. S. Dhesi ⓘ ; V. Novák ⓘ ; R. P. Campion ⓘ ;
K. W. Edmonds ⓘ ; P. Wadley ⓘ

Check for updates

CrossMark

View Online

Export Citation

Articles You May Be Interested In

Staggered field driven domain walls motion in antiferromagnetic heterojunctions

Appl. Phys. Lett. (September 2018)

Spin current detection in antiferromagnetic CuMnAs

Appl. Phys. Lett. (October 2019)

Gating effects in antiferromagnetic CuMnAs

AIP Advances (November 2019)

APL Materials

AIP Publishing

Electrical control of 180° domain walls in an antiferromagnet

View Online   Export Citation   CrossMark

O. J. Amin,[1,a] (ID) S. Reimers,[1,2,3] F. Maccherozzi,[2] S. S. Dhesi,[2] (ID) V. Novák,[4] (ID) R. P. Campion,[1] (ID)
K. W. Edmonds,[1] (ID) and P. Wadley[1] (ID)

AFFILIATIONS

[1] School of Physics and Astronomy, University of Nottingham, Nottingham NG7 2RD, United Kingdom
[2] Diamond Light Source, Chilton OX11 0DE, United Kingdom
[3] Johannes Gutenberg Universität Mainz, Institut für Physik, Staudingerweg 7, 55128 Mainz, Germany
[4] Institute of Physics, Czech Academy of Sciences, Praha 6, 162 00 Prague, Czech Republic

Note: This paper is part of the Special Topic on Emerging Materials in Antiferromagnetic Spintronics.
[a] Author to whom correspondence should be addressed: Oliver.Amin@nottingham.ac.uk

ABSTRACT

We demonstrate the reversible current-induced motion of 180° antiferromagnetic domain walls in a CuMnAs device. By controlling the magnitude and direction of the current pulse, the position of a domain wall can be switched between three distinct pinning sites. The domain wall motion is attributed to a field-like spin–orbit torque that induces the same sense of rotation on each magnetic sublattice, owing to the crystal symmetry of CuMnAs. Domain wall motion is observed for current densities down to $\approx 2.5 \times 10^{10}$ A/m^2 at room temperature.

Antiferromagnets (AFs) offer promising properties for high speed, high density memory applications.[1–3] Antiparallel spin pairs produce no stray fields, meaning AF memory is robust to external fields and there is no device crosstalk. Moreover, AF spin dynamics are typically 2–3 orders of magnitude faster than in ferromagnets.[4,5] Despite their potential, the usefulness of AFs in spintronic devices has been limited by the difficulty controlling the magnetic order using external fields. However, since the prediction of Néel spin–orbit torques (NSOTs) in AF materials,[4] several experimental studies have shown control of AFs using current pulses.[6] Most of these studies have focused on the 90° reorientation of AF domains using orthogonal pulses in four- or eight-contact structures, with an electrical readout via anisotropic magnetoresistance (AMR)[7–14] or spin Hall magnetoresistance (SHMR).[15–20]

A large body of theoretical work has explored driving AF domain walls using various methods, including spin-currents induced by a scanning tunneling microscope tip,[21] spin waves,[22–24] external fields,[25–28] electric field induced anisotropy gradients,[29] and temperature gradients.[30,31] Current-induced NSOTs have been predicted to move AF domain walls with high efficiency and high velocity,[2,32,33] and a combination of x-ray photoemission electron

microscopy (XPEEM) and electrical measurements has revealed the deterministic control of 90° domain walls in CuMnAs.[34] However, there are few examples of 180° domain wall control in antiferromagnets using currents,[35,36] partly because the contribution of 180° AF domain walls to AMR and SHMR is not well understood, making electrical detection difficult.

In this paper, we identify 180° domain walls in CuMnAs thin films and show that they can be controllably moved using electrical current pulses. CuMnAs is an AF material with the required crystal symmetry to enable field-like NSOT on application of electrical current.[4,7]

The magnetic domain structure was imaged using XPEEM combined with x-ray magnetic linear dichroism (XMLD) at the Mn $L_{2,3}$ absorption edge, which shows maximum contrast between domains with Néel vectors collinear and perpendicular to the x-ray linear polarization. By rotating the sample with respect to the x-ray beam, the variation of the AF Néel vector across a 180° domain wall is determined.

A 10 μm wide by 150 μm long curved channel was fabricated from a 50 nm thick layer of CuMnAs epitaxially grown on GaP(001). An optical micrograph of the device is shown in the inset of Fig. 1.
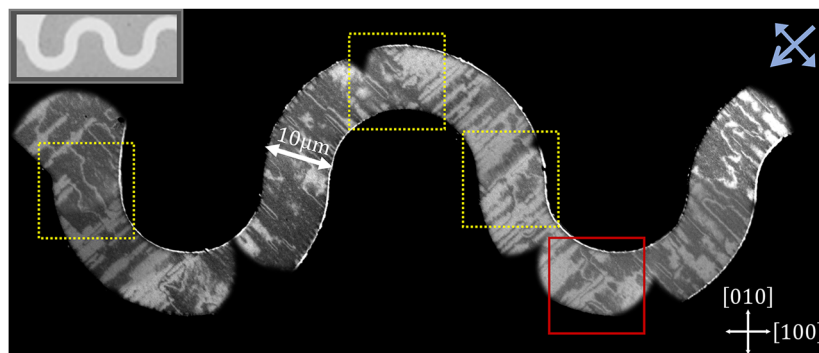
FIG. 1. XPEEM images were stitched together to form an overview of the 10 μm wide channel (optical micrograph inset). Black and white contrast shows antiferromagnetic domains with spin axis oriented along the [1$\bar{1}$0] and [110] crystal axes, perpendicular and parallel to the x-ray polarization (blue double-headed arrow), respectively. Highlighted by the red and yellow boxes are regions where current-induced 180° domain wall movements were seen.

The main panel of Fig. 1 shows a large area map of the antiferromagnetic domain structure of the channel imaged with the incident x-ray polarization along the [1$\bar{1}$0] crystal axis. Domains appear black and white when the Néel vector is perpendicular (along the [110]) and parallel (along the [1$\bar{1}$0]) to the x-ray polarization, respectively. The colored boxes outline regions of the channel where significant current-induced movements of 180° domain walls were observed.

The red box in Fig. 1 outlines a region where a 180° domain wall was controllably moved between three distinct pinning sites using 1 ms wide current pulses. This is shown as a sequence of images in Fig. 2. Figures 2(a) and 2(b) show images for x-ray polarization along [110] and along [100], respectively. The 180° domain walls appear as single-color lines on a background of opposite contrast in Fig. 2(a) and as adjacent black/white lines in Fig. 2(b). The variation of the Néel vector across the domain wall and the resulting XMLD-PEEM contrast are illustrated in Fig. 2(c). From the observed XMLD-PEEM contrast, we can infer that the film has a biaxial magnetic anisotropy with easy axes along the [110] and [1$\bar{1}$0] axes.

Current pulses of 1 ms width and varying amplitude were applied in the directions indicated by the yellow arrows in Figs. 2(a) and 2(b). The initial current pulse of amplitude 15 mA, corresponding to a current density of ≈4 × 10^{10} A/m^2, results in a movement in the position of the domain wall in the center of the image. Subsequent current pulses, applied in the opposite direction, move the domain wall in the opposite direction, with the domain wall position determined by the amplitude and polarity of the pulse.

Figure 3 shows the area moved by the 180° domain wall, relative to the starting position, during a sequence of 16 current pulses of varying amplitude and polarity. Positive current pulse polarity corresponds to pulses along the [100] crystal direction, and negative polarity corresponds to pulses along the [$\bar{1}$00] direction. The wall moves between three distinct stable positions depending on the current pulse applied, with the intermediate state achieved for positive current pulse amplitudes below j_+ = 28 mA. The domain wall motion is observed for current pulse amplitudes as low as j_- = 10 mA (≈2.5 × 10^{10} A/m^2). Finite element calculations of the heating induced by the current are presented in the supplementary material. During a 10 mA 1 ms current pulse, the device temperature increases by less than 10 K, as shown in Fig. S7 of the supplementary material).

While local heating and magnetoelasticity can induce magnetic domain modifications in antiferromagnets, such effects are independent of the polarity of the electrical current.[37] Any thermal gradients induced by the current pulse are also independent of the polarity. Instead, the proposed driving mechanism for the polarity-dependent motion of the 180° domain wall is field-like NSOT. Figure 4 shows a schematic of 180° AF domain wall configurations under the action of a current pulse. Due to the crystal symmetry of CuMnAs, the
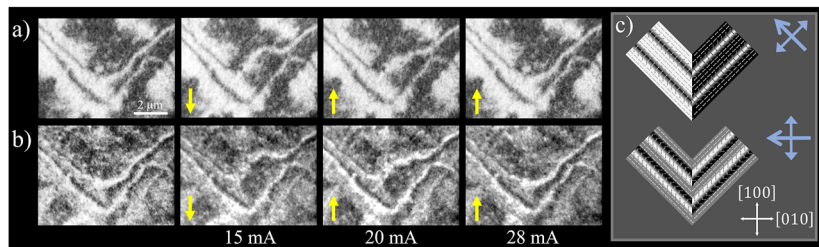
FIG. 2. XPEEM images of the region highlighted by the red box in Fig. 1 with x-ray polarization (blue double-headed arrows) along the (a) [110] and (b) [100] crystal axes. The sequence of images shows a 180° domain wall moving depending on the pulse direction (yellow arrows) and current amplitude. c) A schematic of the Néel vector's (white double-headed arrows) rotation across the domain wall and how that gives rise to different black/white contrasts for the two x-ray polarization directions.
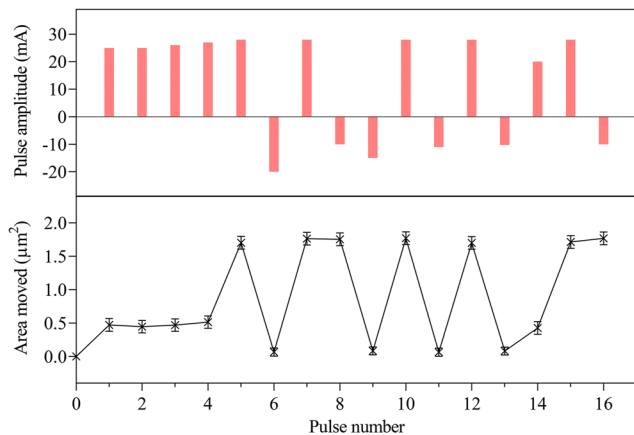
**FIG. 3.** Area moved by a 180° domain wall, relative to the starting position, during a sequence of sixteen 1 ms current pulses. Depending on the current pulse amplitude and polarity, the domain wall can be moved between three pinning sites. Reversing the current pulse polarity causes the domain wall to move in the opposite direction.
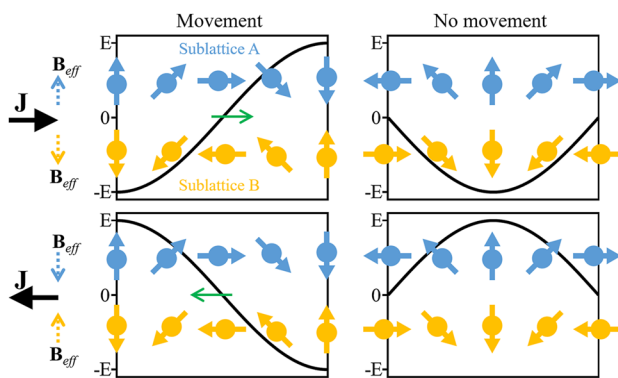

FIG. 4. Antiferromagnetic 180° domain wall configurations that exhibit movement and no movement with an applied current pulse, **J**. The current pulse generates a staggered effective magnetic field, $\mathbf{B}_{eff}$, on the magnetic sublattices (blue and orange dashed arrows), which produces a ponderomotive force, driving the domain wall in the direction indicated by the green arrow. The direction of domain wall movement reverses with a change in the current pulse polarity. In the case of no movement, the current pulse lowers (raises) the domain wall energy, causing it to expand (contract).

current-induced effective magnetic field $\mathbf{B}_{eff}$ is perpendicular to the current direction and alternates sign between the two magnetic sublattices.[4,5,7,38] The field-like NSOT is $\mathbf{T} \sim \mathbf{M} \times \mathbf{B}_{eff}$, where **M** is the sublattice magnetization vector. A ponderomotive force, as a result of the field-like NSOT, drives the domain wall toward the energetically less favorable domain.[2] If the current pulse is parallel/antiparallel to the sublattice magnetization within the domains, no domain wall motion occurs. The current density threshold at which domain wall motion occurs is determined by local strains at the three pinning sites. As presented in Figs. S2 and S5 of the supplementary material, the current density, constrained by the device geometry, in the region of the domain wall movement is non-uniform. The region in which the domain wall movement is observed experiences the largest current density and, hence, the largest field-like NSOT. The lack of movement in other regions of the device (such as the domain wall on the left-hand side of the images in Fig. 2) is, therefore, attributed to the lower current density due to the device geometry, as well as potentially a distribution of domain wall pinning energies.

The exchange interaction between the AF sublattices is much larger than the current-induced NSOT force. This leads to stiff AF domain walls with low effective mass and no Walker breakdown. The upper limit of AF domain wall velocities is determined by the magnon velocity, which is orders of magnitude higher than in FMs.[2,22,32] The results presented demonstrate the ability to control 180° domain walls in an AF via current-induced NSOTs. The direction of movement is determined by the polarity of the applied pulse, and domain walls can be moved between multiple pinning sites depending on the current pulse amplitude. This extends the potential uses of AF materials for low power spintronic devices, allowing for the exploration of AF domain wall velocities, the effects of local defects and strain on depinning energy, and new, high density logic architectures, such as domain wall racetrack.[35,39–41]

AUTHOR DECLARATIONS

Conflict of Interest

The authors have no conflicts to disclose.

Author Contributions

O. J. Amin: Data curation (equal); Formal analysis (equal); Writing – original draft (equal); Writing – review & editing (equal). **S. Reimers**: Data curation (equal); Formal analysis (equal). **F. Maccherozzi**: Data curation (equal); Formal analysis (equal). **S. S. Dhesi**: Data curation (equal); Formal analysis (equal). **V. Novák**: Data curation (equal); Funding acquisition (equal); **R. P. Campion**: Data curation (equal); Funding acquisition (equal). **K. W. Edmonds**: Conceptualization (equal); Data curation (equal); Formal analysis (equal); Funding acquisition (equal); Project administration (equal); Supervision (equal); Writing – original draft (equal); Writing – review & editing (equal). **P. Wadley**: Conceptualization (equal); Data curation (equal); Formal analysis (equal); Funding acquisition (equal); Project administration (equal); Supervision (equal); Writing – original draft (equal); Writing – review & editing (equal).

DATA AVAILABILITY

The data that support the findings of this study are available from the corresponding author upon reasonable request.

REFERENCES

[1]T. Jungwirth, X. Marti, P. Wadley, and J. Wunderlich, "Antiferromagnetic spintronics," Nat. Nanotechnol. **11**(3), 231–241 (2016).

[2]O. Gomonay, T. Jungwirth, and J. Sinova, "High antiferromagnetic domain wall velocity induced by Néel spin-orbit torques," Phys. Rev. Lett. **117**(1), 017202 (2016).

[3]P. E. Roy, R. M. Otxoa, and J. Wunderlich, "Robust picosecond writing of a layered antiferromagnet by staggered spin-orbit fields," Phys. Rev. B **94**(1), 014439 (2016).

[4]J. Železný, H. Gao, K. Výborný, J. Zemen, J. Mašek, A. Manchon, J. Wunderlich, J. Sinova, and T. Jungwirth, "Relativistic Néel-order fields induced by electrical current in antiferromagnets," Phys. Rev. Lett. **113**(15), 157201 (2014).

[5]J. Železný, P. Wadley, K. Olejník, A. Hoffmann, and H. Ohno, "Spin transport and spin torque in antiferromagnetic devices," Nat. Phys. **14**(3), 220–228 (2018).

[6]O.J. Amin, K.W. Edmonds, and P. Wadley, "Electrical control of antiferromagnets for the next generation of computing technology," Appl. Phys. Lett. **117**(1), 010501 (2020).

[7]P. Wadley, B. Howells, J. Železný, C. Andrews, V. Hills, R. P. Campion, V. Novák, K. Olejník, F. Maccherozzi, S. S. Dhesi, S. Y. Martin, T. Wagner, J. Wunderlich, F. Freimuth, Y. Mokrousov, J. Kuneš, J. S. Chauhan, M. J. Grzybowski, A. W. Rushforth, K. W. Edmonds, B. L. Gallagher, and T. Jungwirth, "Electrical switching of an antiferromagnet," Science **351**(6273), 587–590 (2016).

[8]K. Olejník, V. Schuler, X. Martí, V. . Novák, Z. Kašpar, P. Wadley, R. P. Campion, K. W. Edmonds, B. L. Gallagher, J. Garcés, M. Baumgartner, P. Gambardella, and T. Jungwirth, "Antiferromagnetic CuMnAs multi-level memory cell with microelectronic compatibility," Nat. Commun. **8**(1), 15434 (2017).

[9]K. Olejník, T. Seifert, Z. Kašpar, V. Novák, P. Wadley, R. P. Campion, M. Baumgartner, P. Gambardella, P. Němec, J. Wunderlich, J. Sinova, P. Kužel, M. Müller, T. Kampfrath, and T. Jungwirth, "Terahertz electrical writing speed in an antiferromagnetic memory," Sci. Adv. **4**(3), eaar3566 (2018).

[10]S. Y. Bodnar, L. Šmejkal, I. Turek, T. Jungwirth, O. Gomonay, J. Sinova, A. A. Sapozhnik, H.-J. Elmers, M. Kläui, and M. Jourdan, "Writing and reading antiferromagnetic Mn_2Au by Néel spin-orbit torques and large anisotropic magnetoresistance," Nat. Commun. **9**(1), 348–357 (2018).

[11]S. Y. Bodnar, M. Filianina, S. P. Bommanaboyena, T. Forrest, F. Maccherozzi, A. A. Sapozhnik, Y. Skourski, M. Kläui, and M. Jourdan, "Imaging of current induced Néel vector switching in antiferromagnetic Mn_2Au," Phys. Rev. B **99**(14), 140409 (2019).

[12]X. F. Zhou, J. Zhang, F. Li, X. Z. Chen, G. Y. Shi, Y. Z. Tan, Y. D. Gu, M. S. Saleem, H. Q. Wu, F. Pan, and C. Song, "Strong orientation-dependent spin-orbit torque in thin films of the antiferromagnet Mn_2Au," Phys. Rev. Appl. **9**(5), 054028 (2018).

[13]X. F. Zhou, X. Z. Chen, J. Zhang, F. Li, G. Y. Shi, Y. M. Sun, M. S. Saleem, Y. F. You, F. Pan, and C. Song, "From fieldlike torque to antidamping torque in antiferromagnetic Mn_2Au," Phys. Rev. Appl. **11**(5), 054030 (2019).

[14]N. L. Nair, E. Maniv, C. John, S. Doyle, J. Orenstein, and J. G. Analytis, "Electrical switching in a magnetically intercalated transition metal dichalcogenide," Nat. Mater. **19**(2), 153–157 (2020).

[15]X. Chen, R. Zarzuela, J. Zhang, C. Song, X. Zhou, G. Shi, F. Li, H. Zhou, W. Jiang, F. Pan, and Y. Tserkovnyak, "Antidamping-torque-induced switching in biaxial antiferromagnetic insulators," Phys. Rev. Lett. **120**(20), 207204 (2018).

[16]T. Moriyama, K. Oda, T. Ohkochi, M. Kimata, and T. Ono, "Spin torque control of antiferromagnetic moments in NiO," Sci. Rep. **8**(1), 14167 (2018).

[17]L. Baldrati, O. Gomonay, A. Ross, M. Filianina, R. Lebrun, R. Ramos, C. Leveille, F. Fuhrmann, T. R. Forrest, F. Maccherozzi, S. Valencia, F. Kronast, E. Saitoh, J. Sinova, and M. Kläui, "Mechanism of Néel order switching in antiferromagnetic thin films revealed by magnetotransport and direct imaging," Phys. Rev. Lett. **123**(17), 177201 (2019).

[18]P. Zhang, J. Finley, T. Safi, and L. Liu, "Quantitative study on current-induced effect in an antiferromagnet insulator/Pt bilayer film," Phys. Rev. Lett. **123**(24), 247206 (2019).

[19]Y. Cheng, S. Yu, M. Zhu, J. Hwang, and F. Yang, "Electrical switching of tristate antiferromagnetic Néel order in α-Fe_2O_3 epitaxial films," Phys. Rev. Lett. **124**(2), 027202 (2020).

[20]F. Schreiber, L. Baldrati, C. Schmitt, R. Ramos, E. Saitoh, R. Lebrun, and M. Kläui, "Concurrent magneto-optical imaging and magneto-transport readout of electrical switching of insulating antiferromagnetic thin films," Appl. Phys. Lett. **117**, 082401 (2020).

[21]R. Wieser, E. Y. Vedmedenko, and R. Wiesendanger, "Indirect control of antiferromagnetic domain walls with spin current," Phys. Rev. Lett. **106**(6), 067204 (2011).

[22]S. K. Kim, Y. Tserkovnyak, and O. Tchernyshyov, "Propulsion of a domain wall in an antiferromagnet by magnons," Phys. Rev. B **90**(10), 104406 (2014).

[23]E. G. Tveten, A. Qaiumzadeh, and A. Brataas, "Antiferromagnetic domain wall motion induced by spin waves," Phys. Rev. Lett. **112**(14), 147204 (2014).

[24]P. Shen, Y. Tserkovnyak, and S. K. Kim, "Driving a magnetized domain wall in an antiferromagnet by magnons," J. Appl. Phys. **127**(22), 223905 (2020).

[25]O. Gomonay, M. Kläui, and J. Sinova, "Manipulating antiferromagnets with magnetic fields: Ratchet motion of multiple domain walls induced by asymmetric field pulses," Appl. Phys. Lett. **109**(14), 142404 (2016).

[26]K. Pan, L. Xing, H. Y. Yuan, and W. Wang, "Driving chiral domain walls in antiferromagnets using rotating magnetic fields," Phys. Rev. B **97**(18), 184418 (2018).

[27]Z. Y. Chen, Z. R. Yan, Y. L. Zhang, M. H. Qin, Z. Fan, X. B. Lu, X. S. Gao, and J. M. Liu, "Microwave fields driven domain wall motions in antiferromagnetic nanowires," New J. Phys. **20**(6), 063003 (2018).

[28]W. H. Li, Z. Y. Chen, D. L. Wen, D. Y. Chen, Z. Fan, M. Zeng, X. B. Lu, X. S. Gao, and M. H. Qin, "Rotating magnetic field driven antiferromagnetic domain wall motion: Role of Dzyaloshinskii-Moriya interaction," J. Magn. Magn. Mater. **497**, 166051 (2020).

[29]D. L. Wen, Z. Y. Chen, W. H. Li, M. H. Qin, D. Y. Chen, Z. Fan, M. Zeng, X. B. Lu, X. S. Gao, and J.-M. Liu, "Ultralow-loss domain wall motion driven by a magnetocrystalline anisotropy gradient in an antiferromagnetic nanowire," Phys. Rev. Res. **2**(1), 013166 (2020).

[30]S. Selzer, U. Atxitia, U. Ritzmann, D. Hinzke, and U. Nowak, "Inertia-free thermally driven domain-wall motion in antiferromagnets," Phys. Rev. Lett. **117**(10), 107201 (2016).

[31]Z. Yan, Z. Chen, M. Qin, X. Lu, X. Gao, and J. Liu, "Brownian motion and entropic torque driven motion of domain walls in antiferromagnets," Phys. Rev. B **97**(5), 054308 (2018).

[32]T. Shiino, Se-H. Oh, P. M. Haney, S.-W. Lee, G. Go, B.-G. Park, and K.-J. Lee, "Antiferromagnetic domain wall motion driven by spin-orbit torques," Phys. Rev. Lett. **117**(8), 087203 (2016).

[33]Y. L. Zhang, Z. Y. Chen, Z. R. Yan, D. Y. Chen, Z. Fan, and M. H. Qin, "Staggered field driven domain walls motion in antiferromagnetic heterojunctions," Appl. Phys. Lett. **113**(11), 112403 (2018).

[34]P. Wadley, S. Reimers, M. J. Grzybowski, C. Andrews, M. Wang, J. S. Chauhan, B. L. Gallagher, R. P. Campion, K. W. Edmonds, S. S. Dhesi, F. Maccherozzi, V. Novak, J. Wunderlich, and T. Jungwirth, "Current polarity-dependent manipulation of antiferromagnetic domains," Nat. Nanotechnol. **13**(5), 362–365 (2018).

[35]S.-H. Yang, K.-S. Ryu, and S. Parkin, "Domain-wall velocities of up to 750 m s^{-1} driven by exchange-coupling torque in synthetic antiferromagnets," Nat. Nanotechnol. **10**(3), 221–226 (2015).

[36]S. Yu, H. Yoshida, Y. Kotani, K. Toyoki, T. V. A. Nguyen, T. Nakamura, and R. Nakatani, "Antiferromagnetic domain wall creep driven by magnetoelectric effect," APL Mater. **6**(12), 121104 (2018).

[37]H. Meer, F. Schreiber, C. Schmitt, R. Ramos, E. Saitoh, O. Gomonay, J. Sinova, L. Baldrati, and M. Klaui, "Direct imaging of current-induced antiferromagnetic switching revealing a pure thermomagnetoelastic switching mechanism in NiO," Nano Lett. **21**(1), 114 (2021).

[38] X. Zhang, Q. Liu, J.-W. Luo, A. J. Freeman, and A. Zunger, "Hidden spin polarization in inversion-symmetric bulk crystals," Nat. Phys. **10**(5), 387–393 (2014).

[39] S. S. P. Parkin, M. Hayashi, and L. Thomas, "Magnetic domain-wall racetrack memory," Science **320**(5873), 190–194 (2008).

[40] S. Parkin and S.-H. Yang, "Memory on the racetrack," Nat. Nanotechnol. **10**(3), 195–198 (2015).

[41] Z. Luo, A. Hrabec, T. P. Dao, G. Sala, S. Finizio, J. Feng, S. Mayr, J. . Raabe, P. Gambardella, and L. J. Heyderman, "Current-driven magnetic domain-wall logic," Nature **579**(7798), 214–218 (2020).

03 October 2023 12:39:11